Compensation of apparent strain data due to temperature gradients in a full-scale static test of a composite tidal turbine blade

DOI: 10.1784/ndt2023.3a3

Compensation of apparent strain data due to temperature gradients in a full-scale static test of a composite tidal turbine blade

Sara Castellano, Miguel A Valdivia Camacho, Marek J Munko, Fergus Cuthill and Sergio Lopez Dubon
School of Engineering, The University of Edinburgh, The King's Buildings
Edinburgh, EH9 3JL, UK
Sergio.LDubon@ed.ac.uk

Abstract
Composite blades play a crucial role in a tidal turbine's performance, and rigorous testing is required for certification before mass production. This study proposes a methodology for compensating strain measurements affected by temperature gradients using multivariate statistical regressions. This research utilises data analysis and signal processing techniques on strain and temperature datasets obtained from full-scale blade tests at FastBlade, the world's first regenerative fatigue testing facility for tidal turbine blades. The multivariate regression model contains derived coefficients that separate temperature-induced strains from mechanical strains based on strain gauges coupled to their nearest thermocouples available. The linear model's performance is assessed against static test datasets with different temperature conditions and scenarios. The proposed compensation method accurately isolated mechanical strains from high-temperature fluctuations from different sources acting on a large structure, enhancing the reliability of full-scale onshore tidal turbine blade testing.

1. Introduction

1.1 Tidal Energy and Composite Blade Testing

Tidal energy is a form of renewable energy that harnesses the power of ocean tides to generate electricity. It is a promising source of clean and sustainable power which has recently gained traction in the UK, as four projects secured contracts in the fourth round of the government's Contracts for Difference (CfD) scheme, expected to deliver a total of 40.82 MW of capacity[(1)]. Tidal stream turbines designed for most of these tidal projects share similarities with the more mature offshore wind industry, such as the basic three-bladed concept and the components that make these devices. These turbines are expected to operate for 15 years or more under harsh seawater conditions, so composite blades are commonly one of the most critical components.

Developing efficient tidal turbine blades is crucial to maximise energy conversion from the tidal currents. Prior to deploying a turbine array in real-world environments, thorough testing and evaluation are necessary to ensure their performance, durability, and overall safety. Composite blades must be designed to withstand the ultimate design loads and cyclic loading conditions. A blade concept must go through different stages before full-scale prototypes can be tested and thus certified for mass production. Composite blades need to withstand the ultimate design loads as well as design cyclic loads. These full-scale tests can be done in open water facilities like the European

Marine Energy Centre (EMEC) in Orkney, Scotland, or onshore facilities equipped with test rigs. One of these onshore facilities, FastBlade, has achieved a significant milestone by becoming the world's first full-scale regenerative tidal blade fatigue test facility. This achievement is made possible by incorporating a Digital Displacement® hydraulic system, allowing energy recovery during loading cycles at high flow rates[2]. Despite this energy recovery feature, there are no compromises on the quality, control, or confidence in the certification of tidal blades during the testing process.

1.2 Temperature Compensation on Strain Gauges

Strain gauges are the most common way of measuring strain; their fundamental parameter is the sensitivity to strain, known as the Gauge Factor (GF). Their working principle is that they measure the change in electrical resistance, which is proportional to the strain change. Temperature compensation is needed for two reasons. Firstly, the gauge and the specimen to which it is attached will vary according to temperature. The Wheatstone bridge circuit in the gauges will detect the temperature change and return a strain reading. Secondly, the sensitive grating material inside the gauge is also subjected to strain resulting in additional resistance changes.

The effect of thermal output in strain gauges is a widely known phenomenon and has been explored extensively by researchers. Various methods have been proposed to eliminate the undesired effect. K. Choi et al.[3] applied temperature compensation to fibre optic sensors used for measuring the strain of a wind turbine blade. The method consisted of moulding two Fiber Bragg gratings (FBG) in a probe to achieve two different sensitivities for strain and temperature. The true strain is determined by subtracting the temperature effect on the strain signal. Similarly, X. Xiao et al.[4] investigated the factors influencing FBG strain sensors. Additionally, Z. Jin et al. considered the coupling effect of strain gauges and measured objects on thermal output[5]. They developed a temperature compensation method for strain gauges used in asymmetric structures. The study developed a calibration experiment to obtain the thermal output curves relating to the strain gauges and the materials they are attached to. A compensation model was developed to derive the thermal output between two materials with a similar coefficient of thermal expansion. P. Litos et al.[6] developed a computer modelling technique to calculate real thermal strain during a hole drilling strain gauge method to measure residual stresses. S. A. Neild et al.[7] accounted for the thermal output effect using a control strain gauge attached to an unloaded sample of the same material as the test sample, positioned as close as possible so that the samples are under the same environmental conditions. C. Chen et al.[8] researched the effect of temperature on strain measurements using statistical methods, such as linear regression, in box-girder bridges.

Previous work has not yet applied statistical methods on strain measurements of a composite tidal turbine blade. Therefore, this study proposes a novel compensating method for temperature changes in a full-scale static and fatigue test of a tidal turbine blade using statistical regressions considering higher-order temperature behaviour.

The study uses data analysis and signal processing techniques on datasets with no loads applied to the large structure. The strain and temperature data are filtered using a

wavelet transform and down sampled to the same frequency. This is because temperature is logged at a lower frequency than strain. The strain appears to depend on the temperature dynamics; therefore, the compensating model uses a multivariate regression (MVR) to fit the original data and derive the coefficients that could separate the temperature-induced strain from the mechanical strain caused by the applied loads.

2. Materials and Methods

2.1 FastBlade Testing Facility

FastBlade is a research facility designed to test tidal turbine blades and any large, slender structure (2-14 m) under static and fatigue load that fits the reaction frame (see Fig. 1). It can use up to four actuators (only three showing in Fig. 1) attached to saddles and positioned on the blade at different points to achieve an approximate bending moment distribution along the blade under natural environmental conditions.

Figure 1. Experimental setup at FastBlade with three saddles clamped to the blade.

The facility utilises a Digital Displacement® Pumps system that regenerates up to 75% of the energy supplied and with hydraulics allowing up to 1 MN in fatigue load at 1 Hz[(2)]. The efficiency of the hydraulic system translates into rapid test results in weeks rather than months and lower costs for blade developers and clients. Despite this, the mechanical tests last hours or days to test for a full-lifecycle of a tidal turbine blade; this requires large spaces to fit the specimen and for personnel to perform work around the frame. The vastness of the test hall results in temperature fluctuations due to the outside temperature varying or to the central heating system. As it is challenging to keep the temperature stable, the strain gauges are ultimately impacted and will read an apparent deformation due to the temperature changes in the hall.

2.2 Specimen Characteristics

This paper analyses a blade specimen 5.2 m long, weighing 15879 kg and with a natural frequency of 18 Hz. The thickness-to-chord ratio decreased from 55% near the blade root to a minimum of 18% at the tip. The innermost portion of the blade was taken to have a cylindrical cross-section with an implied thickness-to-chord ratio of 100%. The blade was manufactured as part of the DeepGen tidal project, designed by Tidal Generation Limited (TGL) and manufactured by Aviation Enterprises Limited.

The blade skin comprises an 8 mm glass fibre ±45° unidirectional prepreg. The spar is made of carbon fibre unidirectional prepreg, 80% in the longitudinal direction, the rest filled with prepreg in the transverse direction, and a cross-ply woven fabric to provide a bond surface for the shear webs. The shear webs comprise a cross-ply carbon fibre prepreg bonded to the spars. Cross-sectional ribs are 300 mm apart and spread throughout the blade using cross-ply glass fibre prepreg. Finally, a cross-ply glass fibre rear spar is used 100 mm away from the trailing edge to minimise the peel stresses at the skin joint during operation[9].

2.3 Sensor Placement

The strain gauges deformation readings are a crucial section of the data that FastBlade utilises to analyse the specimen behaviour under testing. There are 44 strain gauges (linear and rosette of type FRA-3-350-11, 350 Ω) and 10 K-type thermocouples (TC) with 32 channels positioned on the blade specimen as shown in Fig. 2. The strain gauges are labelled based on their location on the blade and a suffix 0, N45 and P45 as they measure the deformation in the 0º, -45º and +45º, respectively. These strain gauges were paired to their nearest thermocouple, which resulted in 46 unique pairs that showed a strong relationship between the apparent strain and the temperature at every specific location on the blade. The sensor placement can be seen in Fig. 2, which shows the blade specimen with several labelled coordinates. The sensor placement is important due to the temperature fluctuation throughout such a large structure. It should be mentioned that the same methodology is applied to all sensor pairs.

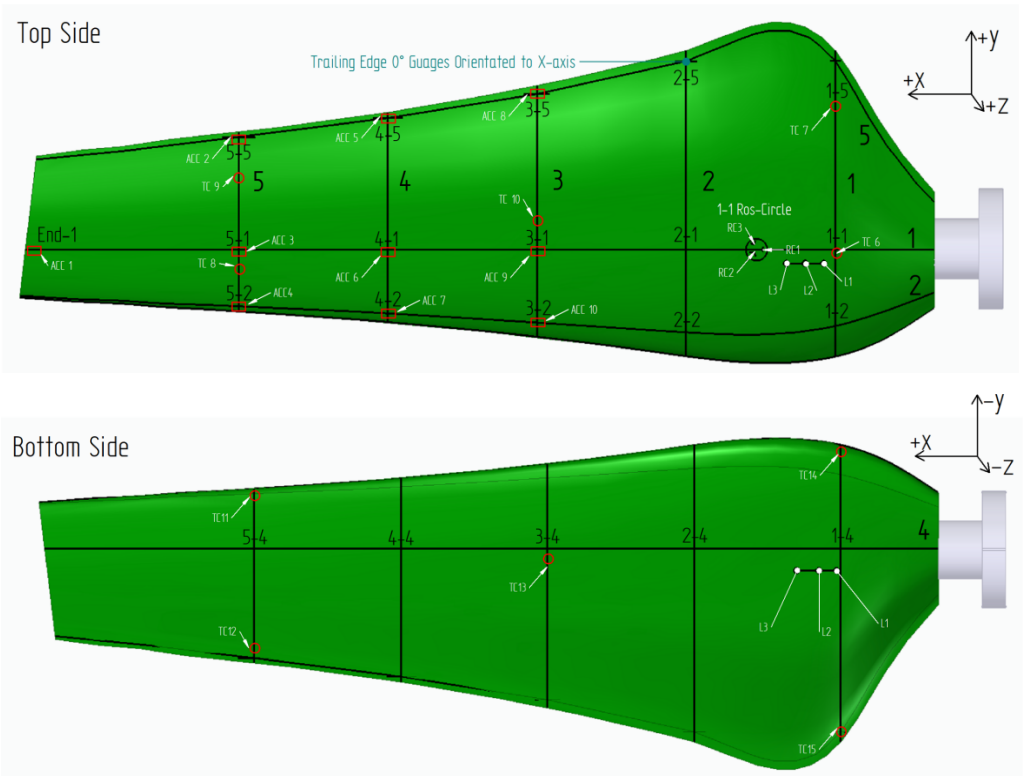

Figure 2. Sensor placement on the blade. The strain gauges are on the black line crossings, and thermocouples are highlighted in red.

The relationship between strain and temperature is derived experimentally using statistical methods. This resulted in 46 pairs with an optimised correlation. The pairs are described in Table 1. Given the negligible distance between the two sensors, nine unique pairs are expected to have the highest correlation value between strain and temperature. These are TC6 with the rosette at 1-1, TC10 with the rosette at 2-1, and TC13 with the rosette at 3-4.

Table 1. List of unique strain gauge and temperature pairs

Thermocouple	Strain gauge
TC6	1-1 (0, N45, P45), 2-1 (0, N45, P45), 1-3 (0)
TC7	2-5 (0)
TC8	4-1 (0, N45, P45). 4-2 (0)
TC9	5-4 (P45)
TC10	2-1 (0, N45, P45), 3-1(0, N45, P45), 4-1(0, N45, P45), 3-2 (0), 3-5 (0)
TC11	5-4 (0, N45, P45)
TC12	5-4 (0, N45, P45)
TC13	2-4 (0, N45, P45), 3-4 (0, N45, P45), 4-3 (0)
TC14	1-4 (0, N45, P45), 2-4 (0, N45, P45), 1-3 (0), 2-3 (0)
TC15	1-4 (0)

2.4 Methodology

2.4.1 Data Acquisition

The data is collected using the National Instrument (NI) data acquisition hardware in TDMS files. This study is based on two no-load temperature tests and three static tests. The temperature tests are run at no-load, meaning that no force is applied to the specimen, and the deformation readings should only result from the temperature changes. The static tests follow the EC TS 62600-3:2020 standard[10]. The datasets and their naming conventions are described in Table 2, along with the ambient temperature range for reference in the no-load temperature tests.

Table 2. Temperature and static test datasets

Name	Description	Ambient temperature range
TM 41	3-day test with no loads applied.	2.59 ºC – 14.69 ºC
TM 42	3-day test with no loads applied.	4.65 ºC – 14.73 ºC
ST 30	Static test with a load of 94 kN per actuator.	N/A
ST 37	Static test with a load of 94 kN per actuator.	N/A
ST 42	Static test with a load of 94 kN per actuator.	N/A

The temperature tests provide two different temperature ranges in the span of three days, which will be differentiated as Temperature Model (TM) 41 and Model 42. Both models experienced a wide range of temperatures to compensate for the temperature effects. For instance, TC6 recorded a range from 5.33 ºC to 25.87 ºC in Model 41 and from 5.73 ºC to 17.14 ºC in Model 42. Figure 3 shows the strong relationship between strain and temperature during three days of recording in the TM 42 for TC6 and 1-1.

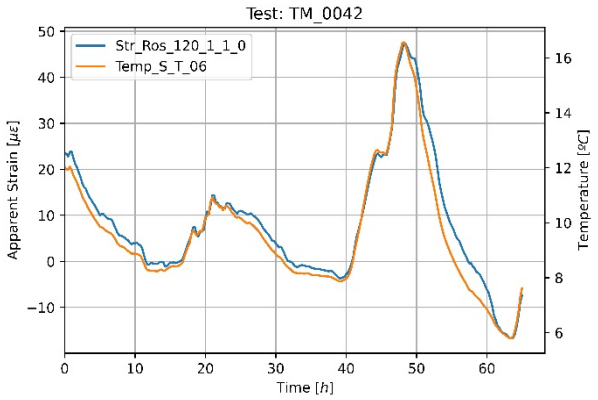

Figure 3. Strain and temperature relationship during a test with no load applied to the large structure.

2.4.2 Data Filtering

In this study, the data is filtered using a wavelet filter. Wavelets are functions that divide the data into several frequency elements and consider each element with a different resolution that matches the scale[11]; researchers tend to use this type of filter because of its advantage over Fourier for signals in dealing with discontinuities. Fourier series states that a function may be represented as a superposition of trigonometric or exponential functions with precise frequencies. However, these functions are not very good at accurately approximating the sharp spikes since they are non-local functions.

2.4.3 Data Resampling

The temperature and strain readings are logged at 25Hz and 100Hz, respectively. This means that to perform any analysis, re-sampling is required. In this study, down-sampling is performed to decrease the size of the signal by reducing the frequency of the data points. Since up-sampling uses interpolation, it creates new data points from new ones. By contrast, down-sampling only utilises existing information, albeit while losing some. This paper selects the down-sampling technique to keep the data as accurate as possible. The down-sampling is performed on the data using the Pandas library[12]; the object must have a date-time index and the re-sampling can be expressed in either frequency or period. The chosen frequency is 1 Hz.

2.4.4 Multivariate Regression Analysis

It became evident that the apparent strain logged during the tests was a combined function of the temperature, the temperature change, and the temperature change rate, in other words, the partial derivatives of temperature. Therefore, the regression fit requires an MVR analysis. The first and second partial derivatives of the temperature and the strain were compared, and a linear regression fit was used to minimise the difference between the predicted and the observed values. The fitting target used in this study is the Sum of Squared Absolute error (SSQABS). The temperature-strain relationship is compared for every TM dataset, and the coefficient with the highest r-squared value is chosen.

$$\varepsilon_t(t) = a \cdot T(t) + b \cdot \frac{dT}{dt}(t) + c \cdot \frac{d^2T}{d^2t}(t) \quad \text{.....(1)}$$

As the slope for every relationship between strain and temperature is found, the strain solely caused by the thermal expansion ε_t can be expressed as in Equation 1. Where *a, b, c* are the slope coefficients, and *T* is the temperature. The behaviour of this equation can be analysed in Figure 4, where the apparent strain *f(t,T)* is compared to the desired mechanical strain *g(t)*, which is independent of the temperature change. The first term of Equation 1 has the most substantial contribution as it compares the instantaneous temperature with the temperature at the start of a test. The second and third terms better capture fluctuations of this fast temperature. At time t_n, the second term of Equation 1 becomes negligible, and the temperature fluctuation is only captured by the third term. On the other hand, at time t_{n+i}, a steady temperature increase is captured only by the second term of Equation 1. Therefore, when a large structure is subjected to temperature fluctuations, the mechanical strain ε_m can be expressed as Equation 2, where ε_a is the apparent strain.

$$\varepsilon_m(t) = \varepsilon_a(t,T) - \varepsilon_t(t) \quad \text{.....(2)}$$

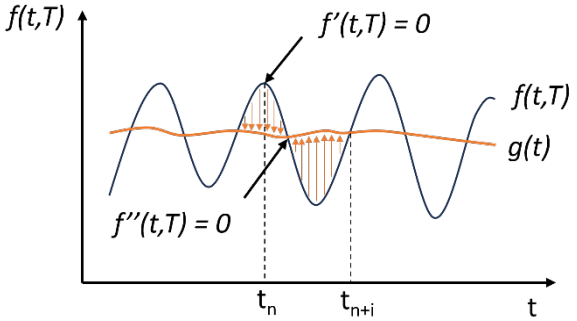

Figure 4. Relationship between the apparent strain (f) and the desired mechanical strain (g) in time and temperature function.

3. Results and Discussion

3.1 Multivariate Regression Analysis

The MVR analysis is performed on TM41 and TM42, following the methodology described in the previous section. As shown in Figure 5, the measured strain still varies when no load is applied to the composite blade. When compared to the temperature data, both measurements show similar shapes in function of time. TM42 shows a stronger relationship between the two channels, whereas TM41 shows changes in the measured strain that the change in temperature cannot explain.

To evaluate the accuracy of both TM tests, the datasets were filtered and down-sampled into 15-minute frequency. The specified period was selected to prioritise the computational performance of the analysis, given the high logging frequency of the strain gauge channels for each test, reaching up to 24 million data points per channel.

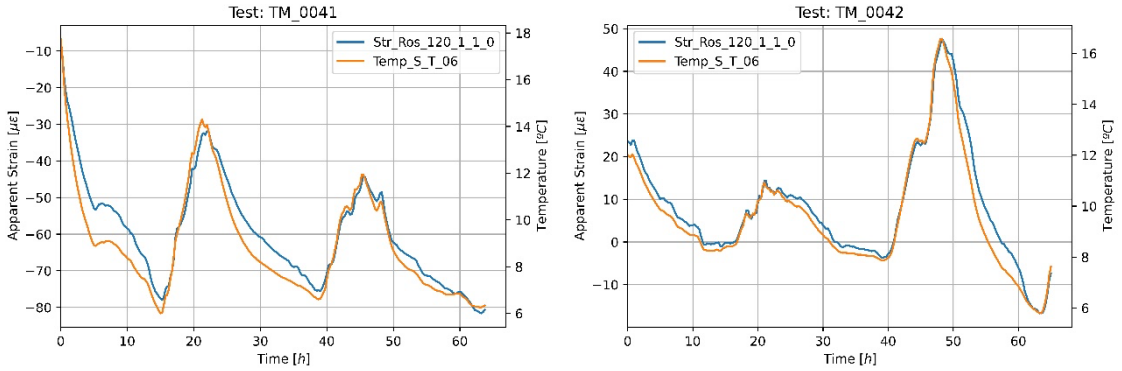

Figure 5. Apparent strain at (a) strain gauge 1-1 and temperature at TC6 in test TM41, (b) strain gauge 3-4 and TC3 in test TM42, with no load applied to the structure.

In Figure 6a, the relationship between temperature and strain at strain gauge 1-1 shows a linear pattern; thus, the slope of the regression equation achieved an r-squared value of 0.971. The instantaneous temperature drifts from approximately -6 ºC to 4.5 ºC. The comparison between the strain gradient and the temperature gradient can be observed in Figure 6b. The cloud of points could also be represented with a linear regression, which resulted in an r-squared value of 0.914. The same procedure was done for the second gradient, thus obtaining the three coefficients for Equation 1. Overall, the regression done for the strain gauge 1-1 on test TM42 showed higher r-squared values and a more accurate representation of the temperature-induced apparent strain.

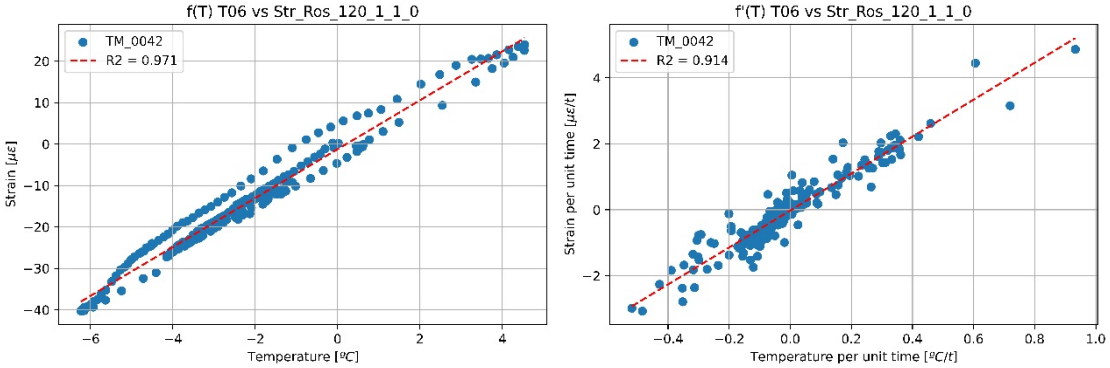

Figure 6. Linear regression analysis at strain gauge 1-1 and TC6 between (a) the change in temperature and strain, (b) the partial derivative of strain and the temperature derivative.

A similar analysis was done with all the unique strain gauges and thermocouple pairs. For instance, the couple between the strain gauge 3-4 (N45) and TC3 also showed a linear behaviour, although with smaller r-squared values. Figure 7a shows one of these comparisons in the test TM42, where the r-squared value for the calculated slope is 0.921. A hysteresis-like pattern can also be observed that could be caused by other external factors as well as the stress recovery rate of the composite. Figure 7b, on the other hand, does not show a cyclic pattern. However, outliers are more predominant. The filtering process might not capture these outliers; thus, another analysis could compare the relationship at different sampling frequencies. The regression slope for the relationship between these two gradients achieves an r-squared value of 0.885.

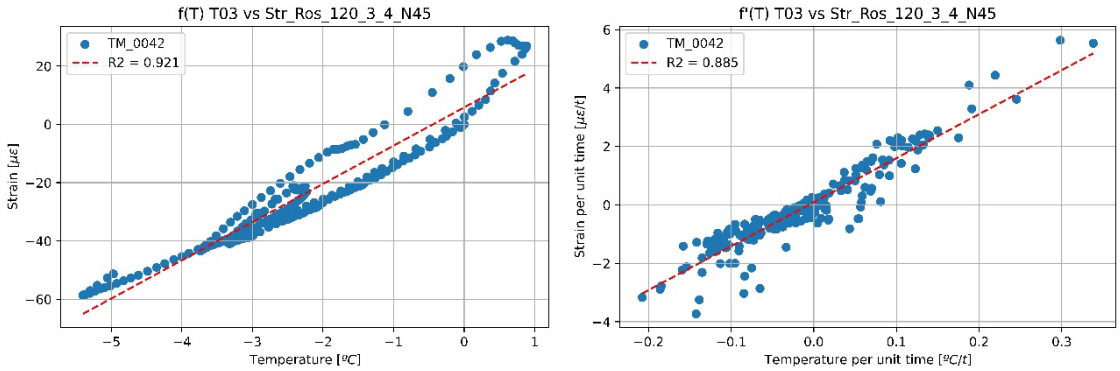

Figure 7. Linear regression analysis at strain gauge 3-4 (N45) and TC3 between (a) the change in temperature and strain, (b) the partial derivative of strain and the derivative of temperature.

3.2 Multivariate Regression Performance

All the most suitable coefficients calculated for every unique pair were stored to apply Equation 2 on the static tests and assess the performance of this MVR analysis. Test ST30 is the test most influenced by the temperature change, as seen in Figure 8a. The highly cyclic temperature change is caused by the heating system, which automatically turns itself on and off based on the ambient temperature. This constant change in conditions visibly biased the data gathered from the strain gauge channel. The load for this test is applied in ramp up from zero to 94 kN in the span of 5 min and a similar ramp down at the end of the test. The load is reflected in the apparent strain data, with two sudden drops at 10:20 and 12:40 caused by external factors unrelated to the temperature fluctuations. Figure 8b shows a closer look at the temperature in TC6 and the strain gauge 1-1, where a relationship between strain and temperature can be observed. The peaks and troughs in this gap would overlap when considering the absolute value of the strain, as this specific location of the composite blade is experiencing a compressive strain.

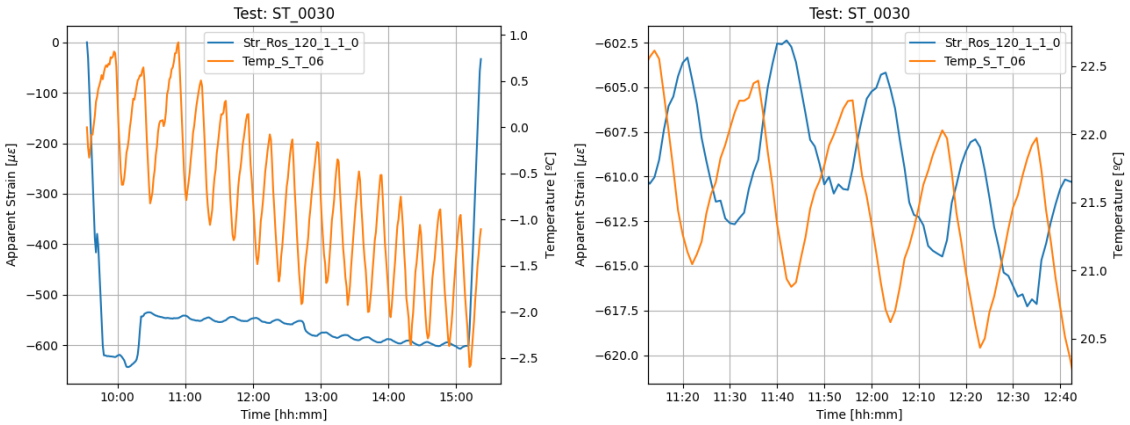

Figure 8. Apparent strain at gauge 1-1 and temperature at TC6 during (a) the entire test ST30, (b) 90 mins of the test.

The second static test available for validation, ST37, was done under a more unpredictable temperature variation, as seen in Figure 9a. The temperature varies by

four ºC over approximately six hours of testing. After 13:30, a sudden drop in temperature is observed, which causes the strain readings at strain gauge 3-1 to start oscillating. An analysis of the gradients of the temperature measurements at TC10 shows the temperature rates oscillating simultaneously with the strain, as seen in Figure 9b. The last static test ST42 is the most stable in temperature change, with only 0.8 ºC between the minimum and maximum recorded ambient temperature. Overall, the regression model showed good behaviour for all possible scenarios of low and high-temperature fluctuations.

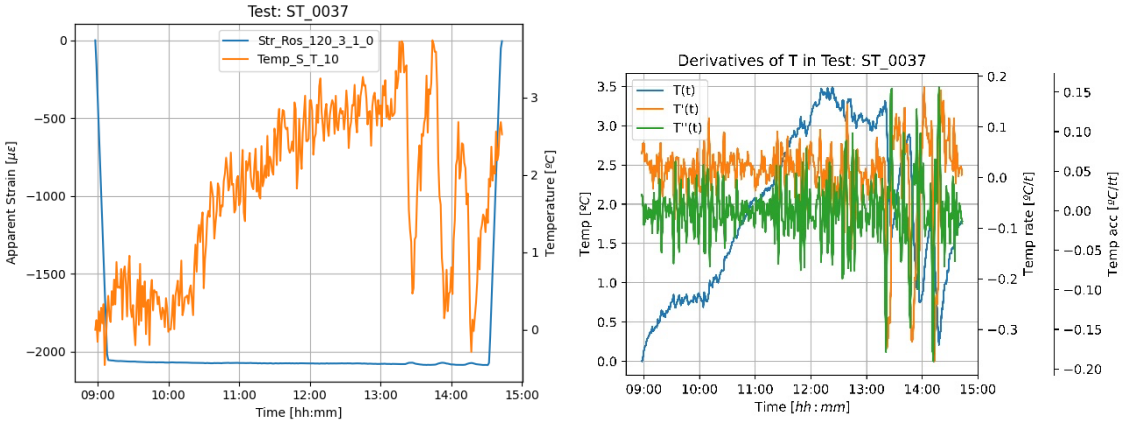

Figure 9. (a) Apparent strain at gauge 3-1 and temperature at TC10 during static test ST37. (b) Temperature gradients at TC10 during static test ST37.

After calculating the temperature-induced strain, the approximate mechanical strain was found using Equation 2 for several pairs proposed throughout all three static tests available. Figure 10a compares the initial apparent strain recorded and the estimated mechanical strain at strain gauge 1-1 for static test ST30. The regression model could effectively suppress the temperature-induced strain from the apparent strain, thus showing a flatter descent before the load is decreased. By comparing the gradient of the new estimated strain and the load coming from the first actuator, the overlap curves effectively prove the accuracy of the resulting strain.

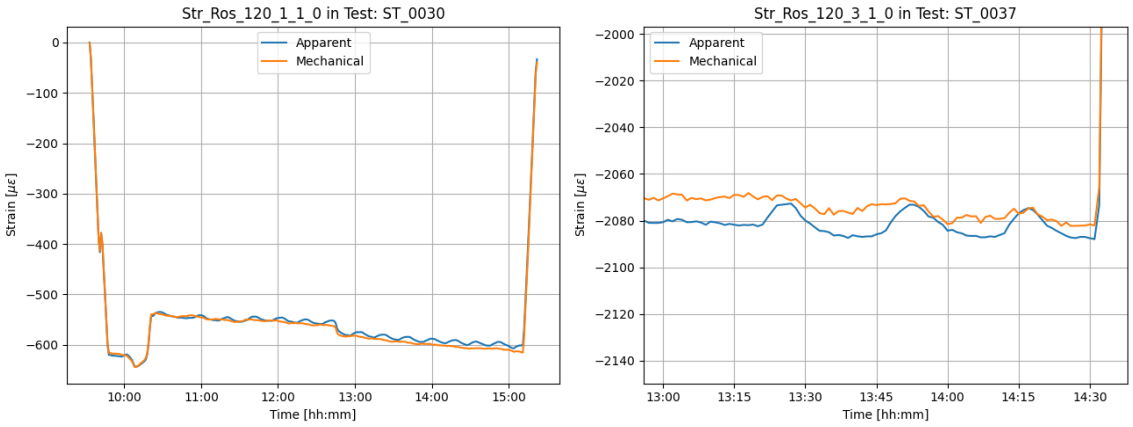

Figure 10. Comparison of apparent strain and mechanical strain for (a) the strain gauge 1-1 in static test ST30 and (b) the strain gauge 3-1 in static test ST37.

Figure 10b shows the result from the same procedure done in Figure 10a for the static test ST37 on the strain gauge 3-1. The regression not only behaves accurately for the first part of the test, where the temperature gradient is slight but also adapts quickly to the sudden drop in temperature starting at 13:20. It can also be observed that the approximation is less accurate when the temperature range is minimal, such as the 4 ºC variation during the static test ST37. This may be caused by the noise level in the temperature signal; thus, a more comprehensive and tailored wavelet filtering must be assessed for every new static test.

For static test ST30, where the temperature fluctuation is mainly determined by the heating system, a pattern based on the location of the strain gauges could be observed. The strain gauges at the top side of the composite blade experienced higher oscillations in their measurements than those at the bottom. This is due to the heating system being at the top of the facility and mild exposure to sunlight from skylights on the ceiling.

4. Conclusions

The mechanical testing of full-scale tidal turbine blades represents several challenges, such as maintaining a stable temperature in the testing facility and across such a large structure under test. These temperature changes affect the strain measurements, resulting in apparent strain due to the thermal output of the lead wire inside the gauge. To solve this problem, a model for temperature compensation is proposed in this paper, which successfully identifies the local statistical coefficients relating strain and temperature that can be applied to the apparent initial readings. The model applies a wavelet filter, resampling, and multivariate regression analysis, which allows the isolation of the temperature effects from the ones due to the applied test loads.

The linear coefficients are obtained from available datasets of two tests on the specimen with no loads applied for three days, where the ambient temperature oscillated between 2.6 ºC and 14.7 ºC. The performance of the multivariate regression model was then assessed with three static tests where a constant load was applied but different temperature conditions. The model successfully obtained the mechanical strain from all the unique pairs of strain gauges and thermocouples. The pairs with the nearest thermocouples available could predict the most accurate results. A high-order multivariate regression could improve the estimations and give results based only on the ambient temperature. The denoising quality also proved to be substantial for static tests where the temperature range is minimal, and lag time intervals could also increase the accuracy of the temperature-induced strain. Overall, the multivariate regression model could quickly adapt to different temperature conditions and accurately detect undesired strains caused by external sources of temperature fluctuation, such as sunlight and artificial heating.

Acknowledgements
Last author: This project has received funding from the European Union's Horizon 2020 research 466 and innovation programme under the Marie Skłodowska-Curie grant agreement No 801215 and 467 the University of Edinburgh Data-Driven Innovation programme, part of the Edinburgh and South 468 East Scotland City Region Deal.

References

1. P Tisheva, Four tidal projects to deliver 41 MW in UK under CfD scheme, Renewables Now, July 2022.
2. S A Lopez Dubon, C R Vogel, D García Cava, F Cuthill, E D McCarthy, and C M Ó Bradaigh, Fastblade: A Technological Facility for Full-Scale Tidal Blade Fatigue Testing, SSRN Electronic Journal, 2023.
3. K S Choi, Y H Huh, I B Kwon, and D J Yoon, A tip deflection calculation method for a wind turbine blade using temperature compensated FBG sensors, Smart Materials and Structures, Vol 21, No 2, January 2012.
4. X Xiao, H Li, H Cui, and X Bao, Evaluation of thermal-drift effect on strain measurement of energy pile, Construction and Building Materials, Vol 362, January 2023.
5. Z Jin, Y Li, D Fan, C Tu, X Wang, and S Dang, Calibration Experiment and Temperature Compensation Method for the Thermal Output of Electrical Resistance Strain Gauges in Health Monitoring of Structures, Symmetry 2023, Vol. 15, Page 1066, Vol 15, No 5, pp10-66, May 2023.
6. P Litoš, M Švantner, and M Honner, Simulation of Strain Gauge Thermal Effects During Residual Stress Hole Drilling Measurements, Vol 40, No 7, pp611–619, October 2005.
7. S A Neild, M S Williams, and P D McFadden, Development of a Vibrating Wire Strain Gauge for Measuring Small Strains in Concrete Beams, Strain, Vol 41, No 1, pp3–9, February 2005.
8. C Chen, Z Wang, Y Wang, T Wang, and Z Luo, Reliability Assessment for PSC Box-Girder Bridges Based on SHM Strain Measurements, Journal of Sensors, Vol 2017 2017.
9. C Huxley-Reynard, J Thake, and G Gibberd, TG-RE-040-0091 Rev B Deepgen Blade Design Report, Bristol, 2008.
10. International Electrotechnical Commission, PD IEC / TS 62600-103: 2018 BSI Standards Publication Marine Energy — Wave, Tidal and Other Water Current Converters, 2018.
11. A Graps, An Introduction to Wavelets, IEEE Computational Science and Engineering, Vol 2, No 2, pp50–61, 1995.
12. W McKinney, pandas: a foundational Python library for data analysis and statistics, Python for high performance and scientific, pp1–9, 2011.